

HIGH TEMPERATURE OXIDATION PROCESS OF P91 STEEL IN CO₂ ATMOSPHERE CONTAINING SO₂

In order to improve the efficiency of power generation system and reduce CO₂ emissions power plants work at high temperature and pressure. Under such conditions modified steel 9Cr, which fulfils the requirements concerning creep resistance, is used. However, Cr₂O₃ formed on the steel does not protect the construction material in the atmosphere which contains CO₂ and SO₂. The aim of the experiment was to study the behaviour of P91 steel in CO₂ atmosphere with the addition of 1% and 5 vol.% of SO₂ at different temperatures (700, 800 and 900°C). It was concluded that the corrosion rate of P91 steel is increasing with a rise in temperature. Scales formed in CO₂ atmosphere at 900°C contain a mixture of iron oxides in the outer layer and chromium-iron spinel in the inner layer. The FeS and Ni were found in the inner zone of scales formed in SO₂ atmosphere.

Keywords: CO₂, scale, SO₂, P91 steel, high temperature oxidation

1. Introduction

In recent years a lot of attention has been paid to increasing the efficiency and reducing emissions in power generation systems, which is connected with an increasing operating temperature and using biomass as a fuel. This causes an additional load on construction materials, which boiler screens, gas turbines, shafts, superheater and reheater tubing are made from; it also accelerates the corrosion process affecting the standard work of the CHP (Cogeneration or combined heat and power) and contributing to a significant increase of operating costs [1,2].

The primary strategy for reducing failure in the power industry is using alloys characterized by high creep strength and increased resistance to thermal fatigue [3]. Currently, 9-12% Cr martensitic steels are the most promising for high temperature applications [4] because of their low thermal expansion coefficient (CTE) and high thermal conductivity [5]. In addition, these alloys are also characterized by resistance to environmental factors.

Typical exhaust gases from power plant consist mainly of CO₂, O₂, H₂O and SO₂ [6]. Sulphur is one of the most aggressive components of flue gases in power boilers. There are several reasons why the corrosion caused by the sulphur-containing atmosphere occurs more rapidly than in the oxidizing environment:

- eutectic temperature in metal-sulphide systems is lower than in the corresponding metal-oxide systems;
- crystalline lattice of sulphides contains more defects in comparison with oxides, which leads to a higher reactivity of reagents [6].

The corrosion rate in sulphur-containing atmosphere depends on the temperature, sulphur concentration and its source (sulphur vapour, SO₂, H₂S, mercaptans) [7].

The degradation rates of steel are higher in the environment containing SO₂ [8], which can be attributed to more defects in metal sulphides in comparison with metal oxides. What is more, they form a low-temperature eutectics in the sulphide system [9]. There are also reports that the presence of SO₂ in the atmosphere hinders the process of Cr₂O₃ formation which has a protective function [10]. Therefore, catastrophic corrosion often takes place in atmospheres containing SO₂.

Several works have been devoted to the study of corrosion process in sulphur-containing atmosphere. Żurek and co-authors examined the influence of SO₂ (0.1, 1.0 and 10.0 vol.%) addition to air atmosphere on Crofer 22APU steel oxidation within the temperature range of 700-900°C. The presence of S was identified only in the outer layer of the scales formed as a result of the oxidation process in atmosphere with SO₂. The authors suggest that the activity of S after SO₂ dissociation is very low for sulphides formation. Additionally, chromium oxide and manganese oxide which formed the scales are very stable and do not react with SO₂ under the conditions studied in the works [11,12]. Kinetics of the oxidation process of Crofer 22APU steel in air with (0.1, 1.0, 10.0 and 20.0 vol.%) SO₂ addition in the temperature range of 700-900°C occurs according to a parabolic law [13]. The oxidation of Cr17Mn17, Cr13Mn19SiCa and Cr15Mn19 steel in SO₂ atmosphere containing 0.01% of oxygen in the temperature range of 800-1000°C also follows the parabolic rate law. Sulphides were found in the inner scale

* CRACOW UNIVERSITY OF TECHNOLOGY, FACULTY OF CHEMICAL ENGINEERING AND TECHNOLOGY, 24 WARSZAWSKA STREET, 31-155, CRACOW, POLAND

Corresponding author: halynakominko@chemia.pk.edu.pl

layer as a result of high activities of metals at the alloy/gas interface in the initial period of the oxidation process and internal transport of SO_2/S_2 [14]. Hua [15] has reported that an increased concentration of SO_2 from 2 to 100 ppm in the water-saturated supercritical CO_2 environment in the presence of 20 ppm O_2 raised the corrosion rate of carbon steel (UNS G15130) from 0.12 mm/year to 0.71 mm/year.

P91 is a 9Cr-1Mo martensitic steel that consists of austenite grains containing packets, blocks, martensite laths and subgrains, which results in good resistance to high-temperature oxidation [16,17]. Therefore, P91 steel is often implemented for the production of tubes, plates and structural components in the power plant industry. According to the producer, P91 steel can be used with permanent operation up to about 650°C [18]. In order to ensure the correct functioning of the equipment in the industrial sector it is important to investigate the effects of higher temperatures and high amount of SO_2 on the oxidation process of steel P91. The aim of the study was to determine the behaviour of P91 steel in CO_2 environment with SO_2 addition (1 and 5 vol.%) in the temperature range of 700-900°C.

2. Materials and methods

Martensitic steel P91 with a composition presented in Table 1 (data from the producer) was selected for the experiment. Samples of the size of 1.0×1.0×0.2 cm were sanded with successive sandpapers down to 2000 grade and then polished by using alumina in order to obtain a mirror-like surface. Next, the sample surfaces were degreased with acetone immediately before the oxidation process and weighed on the analytical balance with accuracy ±0.00002 g. Afterwards, the samples were oxidized.

The experiment was conducted by using a periodic gravimetric method. This method is based on the oxidation of a series of samples under strictly defined thermodynamic conditions and determination of weight gain for each sample over time depending on temperature and gas composition atmosphere.

Steel corrosion gravimetric measurements were performed at 700, 800 and 900°C for 24 hours in air, CO_2 and $\text{CO}_2 + n\text{SO}_2$ ($n = 1$ and 5 vol.%) atmospheres.

TABLE 1

Composition of steel P91

wt. %						ppm				
Fe	Cr	Mn	Mo	Si	Ni	P	S	N	O	C
89.2	9.2	0.7	0.7	0.3	0.3	130	20.0	500	40.0	700

The scheme of the apparatus for the oxidation of steel samples is presented in Fig. 1. The flow rate of each gas fed to the furnace was controlled by flowmeters. The desired temperature was controlled with the aid of a furnace control device.

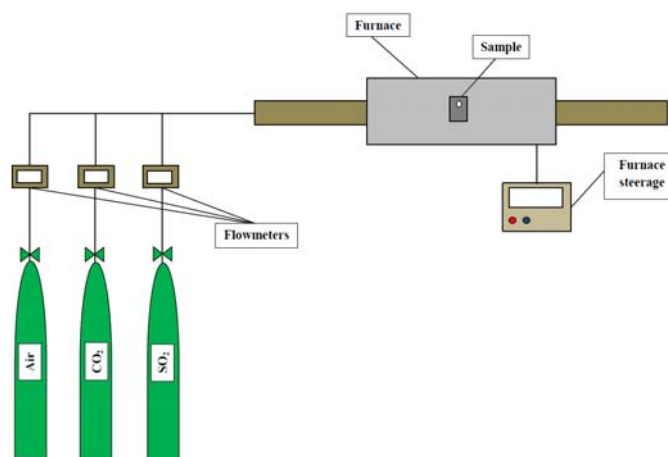


Fig. 1. Scheme of apparatus for oxidation of steel samples

The process of measuring the corrosion rate of the samples included the following stages:

- insertion of the sample into the alund pipe inside the furnace,
- passing Ar to remove the remaining oxygen from the reaction chamber,
- heating the furnace to a desired temperature,
- oxidation process for 24 hours after the stabilization of temperature and setting appropriate gas flow parameters (20 dm³/h),
- cooling in the Ar stream.

For metallographic cross-section preparation the steel samples after oxidation at 900°C were sunk in conductive resin and polished by using automated polishing machine Struers. Next, the metallographic specimens were degreased with ethyl alcohol and used for studying surface morphology of corrosion products by scanning microscope JOEL JSM-6010LA. The phase composition of the obtained oxide scales was determined by using X-ray diffractometer Philips X'Pert.

3. Results and discussion

3.1. Composition of gas atmosphere

In Table 2 the partial vapour pressures of oxygen, sulphur and carbon dioxides in gaseous atmosphere and at different

TABLE 2

Dependence of partial vapor pressures of oxygen, sulphur and carbon dioxides on composition of studied atmospheres

	Air		CO_2		$\text{CO}_2+1 \text{ vol. \% SO}_2$			$\text{CO}_2+5 \text{ vol. \% SO}_2$		
	$p\text{O}_2$ [Pa]	$p\text{CO}_2$ [Pa]	$p\text{O}_2$ [Pa]	$p\text{CO}_2$ [Pa]	$p\text{O}_2$ [Pa]	$p\text{S}_2$ [Pa]	$p\text{CO}_2$ [Pa]	$p\text{O}_2$ [Pa]	$p\text{S}_2$ [Pa]	$p\text{CO}_2$ [Pa]
700°C	$2.0162 \cdot 10^4$	$3.4658 \cdot 10^3$	$5.2003 \cdot 10^{-3}$	$1.0132 \cdot 10^5$	$9.2498 \cdot 10^{-5}$	$7.4961 \cdot 10^{-13}$	$1.0031 \cdot 10^5$	$1.7813 \cdot 10^{-5}$	$5.0537 \cdot 10^{-10}$	$9.6259 \cdot 10^4$
800°C	$2.0159 \cdot 10^4$	$3.4654 \cdot 10^3$	$4.5517 \cdot 10^{-2}$	$1.0132 \cdot 10^5$	$6.9413 \cdot 10^{-3}$	$5.5526 \cdot 10^{-13}$	$1.0031 \cdot 10^5$	$1.4114 \cdot 10^{-3}$	$3.3585 \cdot 10^{-10}$	$9.6259 \cdot 10^4$
900°C	$2.0154 \cdot 10^4$	$3.4654 \cdot 10^3$	$2.7454 \cdot 10^{-1}$	$1.0132 \cdot 10^5$	$1.5650 \cdot 10^{-1}$	$1.0977 \cdot 10^{-12}$	$1.0031 \cdot 10^5$	$4.8999 \cdot 10^{-2}$	$2.8005 \cdot 10^{-10}$	$9.6259 \cdot 10^4$

temperatures are presented. The calculations were done by using FactSage 5.3 programme based on the Gibbs Energy Minimization module for heterogeneous mixtures in equilibrium, and programme's database.

It was found that the oxygen partial vapour pressure decreased by 2 orders of magnitude because of the presence of sulphur dioxide. The partial vapour pressure of oxygen increased with a rise in temperature. Such a tendency was observed in all the studied atmospheres. However, the partial vapour pressure of sulphur was very low; it depended on the concentration of sulphur dioxide in the gaseous mixture and on the temperature. Sulphur partial vapour pressure increased by 2-3 orders of magnitude for each temperature with an increasing SO_2 content in the gaseous mixture from 1 to 5 vol.%. Values of p_{S_2} did not change significantly as a function of temperature. Carbon dioxide concentration in the gaseous mixture did not depend on the composition of atmosphere or on the temperature and it remains almost at the same level.

3.2. Theoretical corrosion products

Using the experimental conditions, as well as the steel and gaseous atmosphere composition, theoretical corrosion products were calculated by using FactSage 5.3 software (Fig. 2a-c). The molar steel/gas ratio used for the simulation was 1/1000, as is recommended by Alviz-Meza [19].

The results of the simulation showed that the main products of scales formed after the oxidation process are Fe_3O_4 (≈ 82 mol.%) and Cr_2FeO_4 (≈ 13 mol.%) in all the simulated atmospheres in the temperature range of 700-900°C.

3.3. Study of the oxidation process of P91 steel

In order to determine the influence of different sulphur dioxide concentrations on the corrosion process of P91 steel the samples were oxidized in air, CO_2 , CO_2+1 vol.% SO_2 , CO_2+5 vol.% SO_2 atmospheres. The results of gravimetric study are presented in Fig. 3 and Fig. 4.

The study showed that the weight gain of P91 steel depends considerably on temperature. The weight gain of samples after oxidation with an increase in temperature was observed in all gaseous mixtures. At 900°C the corrosion process occurred at a high velocity rate, which resulted from a violent weight gain of steel samples after oxidation. In the case of air atmosphere a sample mass increased by 1320 times after oxidation at 900°C in comparison with that at 700°C. A similar situation took place in the case of CO_2+5 vol.% SO_2 , where the weight gain of a sample after oxidation was by 928 times higher at 900°C than at 700°C. However, there was no such a significant impact of temperature on the corrosion rate during oxidation in CO_2 and CO_2+1 vol.% SO_2 atmospheres. There was no sizeable difference between the weight gain of samples at a temperature rise from 700°C to 800°C in the case of CO_2 atmosphere.

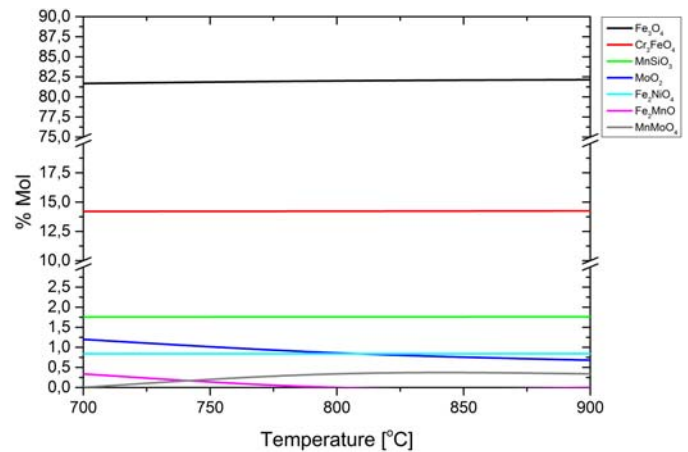


Fig. 2a. Simulated corrosion products after oxidation in CO_2 atmosphere in temperature range 700-900°C

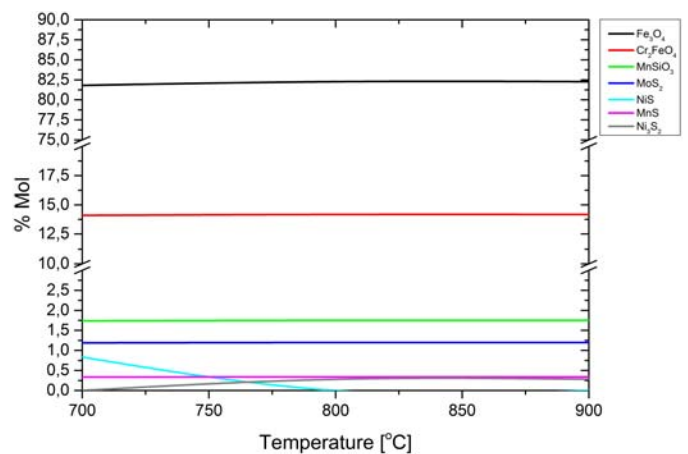


Fig. 2b. Simulated corrosion products after oxidation in CO_2+1 vol.% SO_2 atmosphere in temperature range 700-900°C

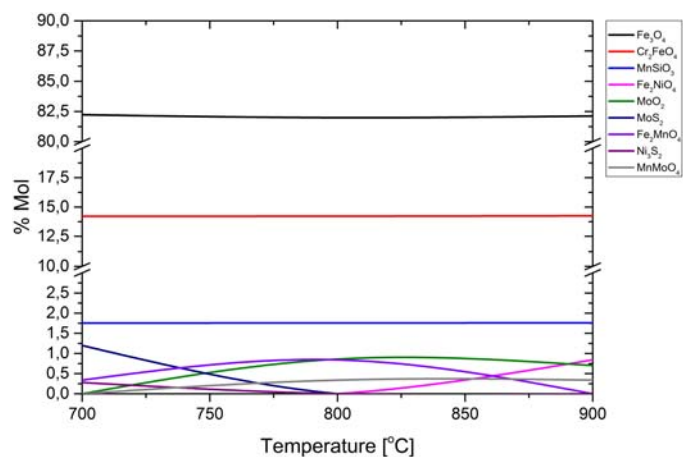


Fig. 2c. Simulated corrosion products after oxidation in CO_2+5 vol.% SO_2 atmosphere in temperature range 700-900°C

The weight gain of steel samples after oxidation in CO_2 atmosphere at 700°C and 800°C was significantly higher than after oxidation in air, while at 900°C there was no difference in weight gain after oxidation in CO_2 and air atmospheres. The addition of SO_2 to CO_2 atmosphere accelerated the corrosion rate of P91 steel in comparison with air. Nevertheless, the

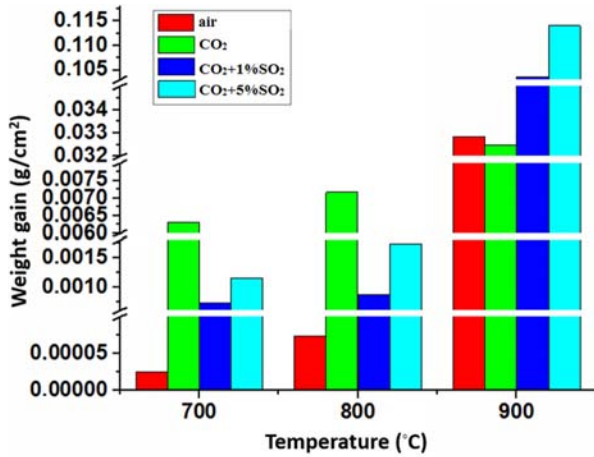


Fig. 3. Dependence of weight gain of steel samples on temperature

weight gains of samples after oxidation in CO_2+1 vol.% SO_2 and CO_2+5 vol.% SO_2 at 700°C and 800°C were lower than in CO_2 atmosphere. Such a phenomenon can be attributed to the fact that the partial pressure of atomic oxygen, which occurs in the oxidation reaction, is higher in CO_2 atmosphere in comparison with the atmosphere containing SO_2 . Therefore, the oxidation process in CO_2 atmosphere is faster.

At 900°C the oxidation process of P91 steel proceeded faster in atmospheres containing SO_2 in comparison with CO_2 atmosphere and the weight gain of samples tended to increase after oxidation with increasing SO_2 content.

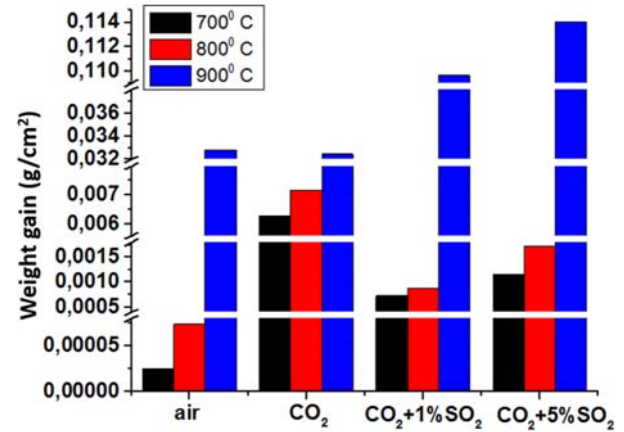


Fig. 4. Dependence of weight gain of steel samples on gas composition of atmosphere

3.4. Study of phase composition of scales

Results of XRD study of scales formed after oxidation in air, CO_2 , CO_2+1 vol.% SO_2 and CO_2+5 vol.% SO_2 atmospheres are presented in Fig. 5.

An X-ray analysis showed that the scales formed in air at 800°C (Fig. 5a) and 900°C consisted of iron oxide (Fe_3O_4). The scales obtained after the oxidation process in CO_2 atmosphere at 700°C and 900°C were identified as haematite (Fe_2O_3) and magnetite (Fe_3O_4), while at 800°C chromium-iron spinel was formed (Fig. 5b). Products of the oxidation reaction in gaseous

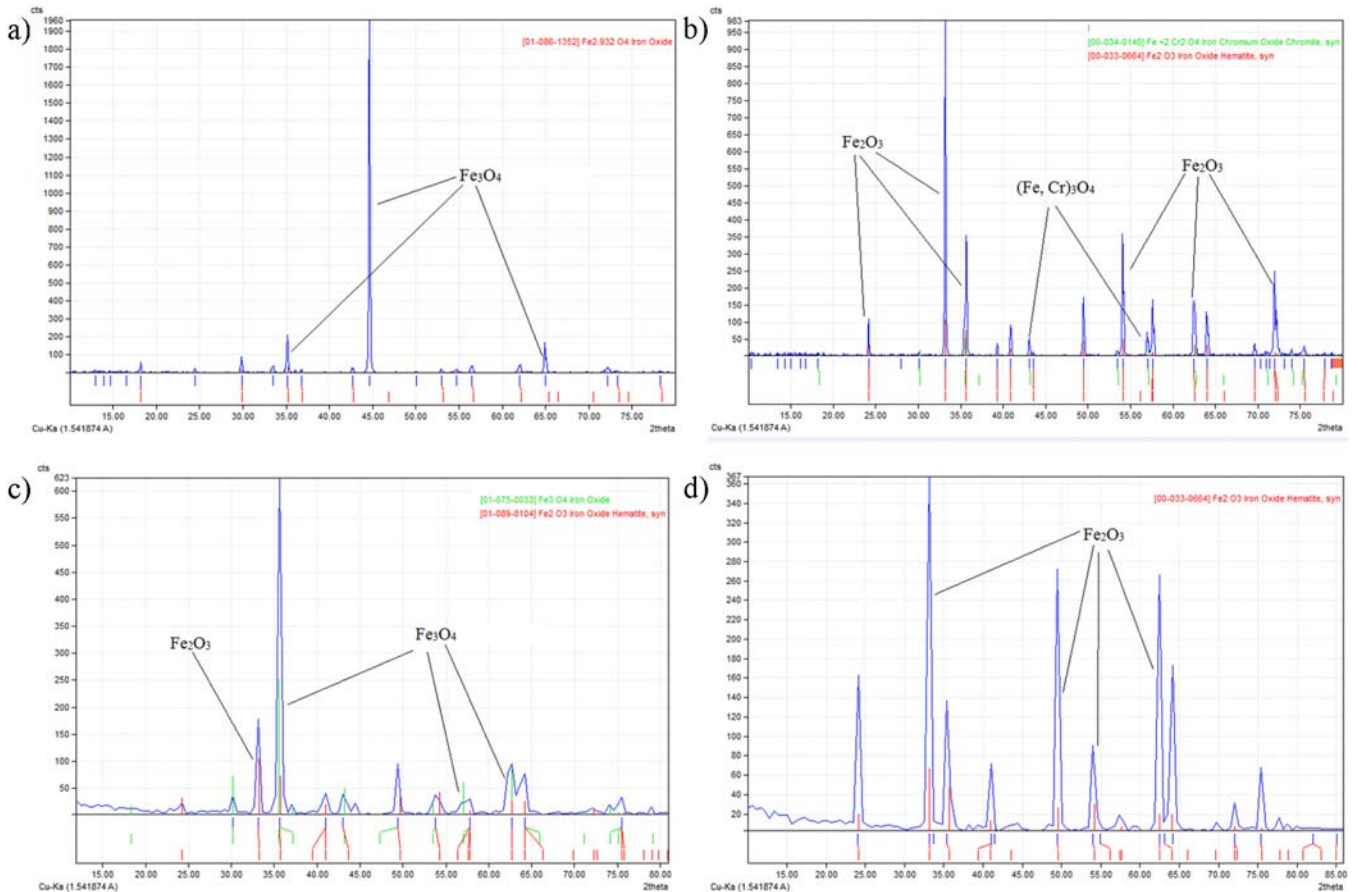


Fig. 5. Results of XRD study. a – air (800°C), b – CO_2 (800°C), c – CO_2+5 vol.% SO_2 (700°C), d – CO_2+1 vol.% SO_2 (800°C)

TABLE 3

Thickness of scales formed at 900°C in different atmospheres

Atmosphere	Scales thickness, μm
CO_2	200
$\text{CO}_2+1 \text{ vol.}\% \text{ SO}_2$	500
$\text{CO}_2+5 \text{ vol.}\% \text{ SO}_2$	1200

mixtures with SO_2 addition contained iron oxides (Fe_2O_3 , Fe_3O_4) in the case of 1 vol.% of SO_2 at 900°C as well as in the presence of 5 vol.% of SO_2 at 700°C (Fig. 5c). The composition of scales formed after oxidation in $\text{CO}_2+1 \text{ vol.}\% \text{ SO}_2$ at 700°C and 800°C was identified as haematite (Fig. 5d). The same structure had products formed in $\text{CO}_2+5 \text{ vol.}\% \text{ SO}_2$ atmosphere at 800°C and 900°C.

The surfaces of scales and metallographic specimens prepared from the samples after oxidation at 900°C in CO_2 , $\text{CO}_2+1 \text{ vol.}\% \text{ SO}_2$ and $\text{CO}_2+5 \text{ vol.}\% \text{ SO}_2$ atmospheres were subjected to scanning microscopy in order to identify the composition and structure of the scales. The study showed that the scales morphology changed with the changing composition of gaseous mixtures. The scale formed after oxidation in CO_2 atmosphere was coarse-grained, while the addition of SO_2 to atmospheres resulted in the formation of more compact scales (Fig. 6).

SEM images showed that the outer layers of the scales formed after oxidation at 900°C in CO_2 , $\text{CO}_2+1 \text{ vol.}\% \text{ SO}_2$ and $\text{CO}_2+5 \text{ vol.}\% \text{ SO}_2$ atmospheres consisted of Fe and O, which confirmed the results of the XRD study.

Thickness of the scales was a function of SO_2 concentration in gaseous mixtures (Table 3). The addition of 1 vol.% of SO_2 resulted in an increase of scales thickness by 150% in comparison with the scale formed in CO_2 atmosphere. In the case of 5 vol.% of SO_2 the thickness of scale was by 500% bigger than in CO_2 atmosphere.

The scales (Fig. 7) formed as a result of oxidation reaction in air, CO_2 , $\text{CO}_2+1 \text{ vol.}\% \text{ SO}_2$ and $\text{CO}_2+5 \text{ vol.}\% \text{ SO}_2$ at 700°C and 800°C had good adhesion to metallic core, while the products obtained at 900°C were fragile, cracked and spalling.

The results of scanning electron microscopy allowed to conclude that the scale formed in CO_2 atmosphere at 900°C consisted of two layers and the thickness of each was approximately 100 μm (Fig. 7a). It was found that the outer layer contained Fe_2O_3 and Fe_3O_4 , whereas in the inner layer chromium-iron spinel was identified. Spinels of Ni were observed in the inner layer of the scale formed in CO_2 atmosphere. Scales obtained in gaseous atmospheres with SO_2 addition contained three layers – a compact outer layer, a porous inner layer and a thin layer of internal oxidation zone which adhered to the metallic core. Outer layers of scales formed in $\text{CO}_2+1 \text{ vol.}\% \text{ SO}_2$ and $\text{CO}_2+5 \text{ vol.}\% \text{ SO}_2$ at 900°C consisted of a mixture of iron oxides (Fig. 7b,7c). The chromium-iron spinel was found as a component of an inner layer of scales obtained after oxidation in gaseous atmospheres

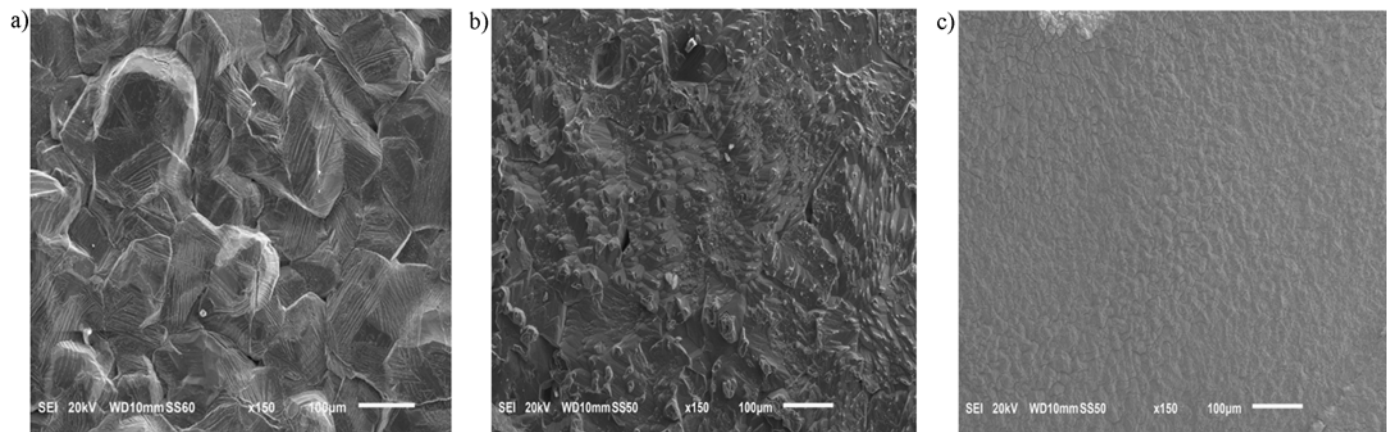


Fig. 6. Morphology (SEM) of scales surface. a – CO_2 (900°C), b – $\text{CO}_2+1 \text{ vol.}\% \text{ SO}_2$ (900°C), c – $\text{CO}_2+5 \text{ vol.}\% \text{ SO}_2$ (900°C)

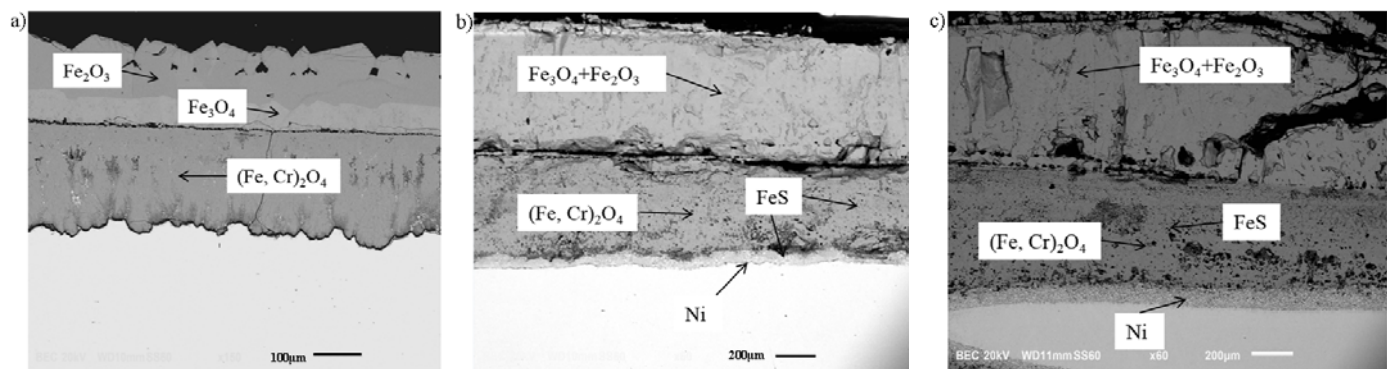


Fig. 7. SEM cross sections of scales. a – CO_2 (900°C), b – $\text{CO}_2+1 \text{ vol.}\% \text{ SO}_2$ (900°C), c – $\text{CO}_2+5 \text{ vol.}\% \text{ SO}_2$ (900°C)

with SO₂ addition. These results coincide with the results of a simulation, where the Fe-based oxides and Fe-Cr spinel were the main products of corrosion. The analysis of Ellingham-Richardson diagram [20] confirmed that haematite and magnetite formed after oxidation in air, CO₂ and CO₂ + nSO₂ (n = 1 and 5 vol.%) atmospheres are thermodynamically stable at all the studied temperatures.

SEM/EDS analysis showed the presence of S in the inner layer of the scales formed in CO₂ atmospheres with SO₂ addition. Due to Ellingham-Richardson diagram for sulphides [20] in the temperature range of 700-900°C, the partial vapour pressure of S₂ (between 10⁻¹²-10⁻¹¹ atm) is lower than the dissociation pressure of FeS (between 10⁻⁹-10⁻⁸ atm.), as a result FeS cannot be formed. However, the partial vapour pressure of S₂ in the scale is usually higher than that at the scale/gas interface, which allows for the FeS formation. Two possibilities of FeS formation can be considered: 1) direct transport of SO₂ molecules from the gas phase through the oxide scale, or 2) oxidation of transient sulphide to SO₂ can take place [21]. The formation of FeS as a result of sulphur diffusion towards the core during the oxidation process was suggested in the study conducted by [14], where Cr13Mn18Si2Ca and Cr17Mn17 were oxidized for 14 hours in SO₂ atmosphere and for subsequent 4 hours in ³⁵SO₂ at 1173 K. Olszewski [5] reported that the presence of FeS in the scale facilitates the outward diffusion of iron, which accelerates the oxidation process.

4. Conclusions

The study of oxidation of P91 steel in air, CO₂ and CO₂ + nSO₂ (n = 1, 5 vol.% SO₂) atmospheres at 700, 800 and 900°C was performed. It can be stated that:

- the presence of SO₂ accelerates the corrosion process at 900°C. However, at 700 and 800°C higher weight gains of samples were observed in the case of CO₂ atmosphere;
- an increase of SO₂ in the gaseous mixture leads to the formation of more compact scales;
- in CO₂ atmosphere at 900°C the oxidation product consists of two layers – outer, which contains a mix of iron oxides, and inner, identified as chromium-iron spinel;
- when the atmosphere contains SO₂ three layers of scale were formed (outer, inner, and zone of internal oxidation). The formation of FeS in the inner layer proves sulphur diffusion towards the core during the oxidation process;
- thickness of scales formed after oxidation is a function of SO₂ concentration in the gaseous mixture.

REFERENCES

- [1] C.P. O'Hagan, B.J. O'Brien, S.B. Leen, R.F.D. Monaghan, *Corros. Sci.* **109**, 101-114 (2016).
- [2] C. Mobbs, *Guidelines/guidance by source category: Part III of Annex C*, Victoria, Australia (2006).
- [3] J. Ehlers, D.J. Young, E.J. Smaardijk, A.K. Tyagi, H.J. Penkalla, L. Singheiser, W.J. Quadackers, *Corros. Sci.* **48**, 3428-3454 (2006).
- [4] C. Pandey, A. Giri, M.M. Mahapatha, *Materials Sciences & Engineering A* **664**, 58-74 (2016).
- [5] T. Olszewski, *Tag der mündlichen Prüfung*: 15.08.2012.
- [6] W. Schulz, M. Nofz, M. Feigl, I. Dorfel, R. Saliwan Neumann, A. Kranzmann, *Corros. Sci.* **68**, 44-50 (2013).
- [7] M. Homa, *Instytut Odlewnictwa, Kraków* **48**, 4, 19-41 (2008).
- [8] Y. Xiang, M. Xu, Y.-S. Choi, *Corrosion Engineering, Science and Technology* **52** (7), 485-509 (2017).
- [9] A. Radziszewska, A. Kranzmann, I. Dörfel, M. Mosquera Feijoo, M. Solecka, *Arch. Metall. Mater.* **61**, 1607-1612 (2016).
- [10] Z. Grzesik, A. Poczekajło, A. Kaczmarek, S. Mrowiec, *Ochrona przed korozją* **54** (6), 341-343 (2011).
- [11] Z. Żurek, A. Jaroń, M. Homa, *Oxid. Me.* **76**, 273-285 (2011).
- [12] Z. Żurek, J. Gilewicz-Wolter, A. Jaroń, M. Homa, *Ochrona przed korozją* **54** (6) 330-332 (2011).
- [13] Z. Żurek, J. Gilewicz-Wolter, M. Hetmańczyk, J. Dudała, *Inżynieria materiałowa*, 1 (138), Styczeń-Luty (2004).
- [14] Z. Żurek, J. Gilewicz-Wolter, M. Hetmańczyk, J. Dudała, A. Stawiarski, *Oxid. Met.* **64** (5/6), 379-395 (2005).
- [15] Y. Hua, R. Barker, A. Neville, *Corrosion* **71** (5), 667-683 (2015).
- [16] K. Makowska, L. Piotrowski, Z.L. Kowalewski, J. Nondestruct. Eval. **36** (43), 10 (2017).
- [17] M. Thirupathy, S.Z. Mazharuddin, S. Biswas, *Int. J. Chem. Tech. Res.* **7** (2), (2014).
- [18] ThyssenKrupp Materials International. *Material data sheet P91/T91* (2011).
- [19] A. Alviz-Meza, J.A. Sanabria-Cala, V. Kafarov, D.Y. Pena-Ballesteros, *Chemical Engineering Transactions* **70**, 1069-1074 (2018).
- [20] L.L. Shreir, R.A. Jarman, G.T. Burstein, *Corrosion 1, Metal/Environment reactions*. Butterworth-Heinemann 2000.
- [21] P. Huczowski, T. Olszewski, M. Schiek, B. Lutz, G.R. Holcomb, V. Shemet, W. Nowak, G.H. Meier, L. Singheiser, W.J. Quadackers, *Materials and Corrosion* **65** (2), 121-130 (2014).